International Journal of Advanced Technology and Engineering Exploration, Vol 11(117)
ISSN (Print): 2394-5443 ISSN (Online): 2394-7454
http://dx.doi.org/10.19101/IJATEE.2023.10102571

Research Article

Finite element analysis of failure at the aluminium-carbon fiber composite

Amol Rasane[1*], Prashant Kumar[2] and Mohan Khond[2]
Assistant Professor, Department of Mechanical Engineering, PVG's College of Engineering & S.S. Dhamankar Institute of Management, Nashik, Maharashtra, India[1]
COEP Technological University, Pune, Maharashtra, India[2]

Received: 04-December-2023; Revised: 23-August-2024; Accepted: 26-August-2024

Abstract
The aluminium alloy is used for fabricating structural components in aeroplanes. The development of cracks and their propagation is a cause of concern because it may lead to failure of the structure if the crack undergoes an uncontrolled growth. The composite patching has been successfully used for repairing cracks in secondary load carrying structures of aeroplanes. A composite patch when bonded to the cracked region increases the strength of the structure and prevents the growth of the crack front. But the adhered patch separates at the bonding surface because of external loads. Mechanism by which this separation occurs is still not well understood and an investigation of the same is carried out in this research. The experiments were performed by subjecting the patched specimen to external tensile loads. But the experiments only give the load at which the specimen fails. For understanding the separation process, numerical simulation was performed in Ansys program by employing finite element method (FEM) and cohesive zone model (CZM). Instantaneous values of the loads, separation distance and the separation areas were obtained at different stages of loading and they were compared with their critical values. The composite patch begins to separate at low loads because of simultaneously acting normal (peel) and perpendicular (shear) stresses. Speed at which separation occurs increases once the yield stress is exceeded and at high values of external loads, the patch separates completely from the substrate.

Keywords
Crack repair, Composite patch, Patch separation, Finite element method, Cohesive zone model.

1.Introduction
Thin aluminium sheets find usage in several industries that include construction, automobile and aircraft companies. These structures may be exposed to damages and defects in their service lives because of the structural loads acting on them. Due to these loads, the panels are subjected to stresses that elevate at high magnitudes of external load. These elevated stresses result in damage, mostly in the form of cracks. If these cracks go unnoticed, they have a tendency to grow rapidly beyond the threshold limit. Early detection of cracks through proper inspection can help in implementing appropriate measures for preventing crack growth and the resultant failure. Ratwani in 2000 [1] elaborated on the repair options for damaged aircraft structures and discussed various structural life enhancement methods. Marazani et al. in 2017 [2] carried out a comprehensive review of the methods of crack repair in metals and proved that the composite patching is a better alternative than the traditional methods for repairing cracks in thin metal sheets.

The traditionally employed measures for repairing cracks include the use of mechanical fasteners and welding of a metal patch. Though advantageous in terms of execution, these traditional methods pose inherent disadvantages in the form of stress concentration in fastening and thermal stress is the case of welding which reduces the effectiveness of the repair. A simple and effective measure is repairing by composite patching method, which offers advantages over the traditional techniques in terms of material availability, ease of operation and strength to weight ratio. Originally developed for military aircraft maintenance, this method was later extended to civil aircraft as well. The composite patching technique has been employed in several researches, the prominent among them being Baker in 1988 [3], Baker et al. in 2003 [4] and Duong and Wang in 2010 [5]. With substantially less stress concentration than mechanical fastening, the patch with high strength and high modulus is able to transfer the stresses uniformly and effectively between the aluminium panel and composite patch. Because of its inherent nature of offering flexibility; the patch made of composite

*Author for correspondence

material containing fiber and resin as its constituents can be applied even to a structure with surface irregularities. The researchers Sun et al. in 1996 [6] and Rastogi et al. in 1998 [7] found the composite patching as an effective technique for repairing cracks in thin sheets. Colombi et al. in 2003 [8] applied the composite patching technique for the repair of a cracked steel plate used in the riveted steel bridges and found that patch stiffness does not affect the release of energy during debonding. Okafor et al. in 2005 [9] reported that the patch considerably reduces peak stress in thin cracked sheets by undertaking durability study.

Davis et al. in 2006 [10] carried out an in-depth study of adhesively bonded technology and relevant standards for composite repair of old aircrafts and emphasized that surface preparation is important for an effective repair. Liu et al. in 2007 [11] through comparisons with the experimental results proposed a theoretical model that proved effective in providing an accurate estimation of the crack growth. Thus, crack repair using composite patch has been proved effective in avoiding the failure of the structural sheets. The composite patch can be applied on both sides of the cracked region in a two-sided method, preventing further crack propagation. Practically, availability of one of the two sides of metal panel makes the usage of one-sided patch imperative. The asymmetry of the patch results in stresses at the interface that are developed due to induced bending moment. Once the separation of the patch is initiated, it continues at a rapid rate with the increasing external load. Ultimately, the patch separates completely from the substrate and exposes the crack beneath to the external loads. The crack front then grows exponentially, leading to breakage of the structure into distinct pieces. The geometrical parameters i.e. patch length, width and thickness plays a significant role in failure of patch. It is thus important to know the mechanism by which the patch gets debonded from the surface so that appropriate measures can be incorporated to avoid the separation of the patch and prevent the failure of the structure.

1.1Challenges

The debonding at the contact surface is responsible for failure of the patch and ultimately breakage of the panel. This separation occurs through a complex mechanism involving nonlinear effects of geometry and materials. Kwon and Lee in 2013 [12] performed the analysis of the crack repair using a composite patch with the help of an analytical model. The model could predict the linear behaviour of the patched system at low loads but could not predict its behaviour when the complexities were increased at high loads. Khan and Essaheb in 2017 [13] experimentally investigated the behaviour of a growing crack for an aluminium sheet with a notch adhered with a composite patch. The experiments only give stress to failure and its location and the mechanism of patch failure cannot be known only by performing experiments. The use of advanced computational tools involving capabilities of modelling non-linear effects and complex contact analysis become imperative. Ramji and Srilakshmi in 2012 [14] carried out an investigation of the performance of crack repair by determining stress intensity factor (SIF) using finite element method (FEM). Through this method, linear behaviour of patch repair could be understood but it is not effective when complexities involving nonlinearities are to be considered. Thus, the approaches employed in the earlier studies could not help to understand the failure mechanism of the composite patch. Advanced computational tools such as contact analysis help in analysing complex behaviour during interface separation but it is a time-consuming process which involves monitoring of stresses, displacements and energy values at various instances. This kind of analysis is performed for a number of different combinations by varying the geometrical parameters of the patch. Further post-processing is required for determining the separated area in which the nodes were separated as per the failure criterion.

1.2Motivation

The composite patching can be used for applications using thin metal panels as the materials required for the repair are easily available and the method of repair can be easily executed. The understanding of failure mechanisms in composite repair can help in redesigning the patch geometry with an appropriate combination of length, width and thickness. This would enhance the life of the structure and result in fail-safe working conditions during its service.

1.3Objectives

To comprehend the complex failure process occurring at aluminium-composite interface in repair of center crack in thin aluminium alloy sheet using carbon fiber composite patch.

The detailed stress analysis has been carried out using advanced techniques such as FEM and cohesive zone material (CZM) model at the contacting surfaces. The study being fundamental in nature has helped in understanding the complex behaviour of metal-composite interface and also in determining an

appropriate geometry of the patch for an improved performance.

The remaining part of the manuscript is organized as follows: the research carried out on crack repair using composite patch by earlier researchers is reviewed in Section 2. Section 3 describes experimental and numerical methods employed for the study of patch failure. A comprehensive discussion on results obtained in experiments and through simulations along with the outcomes is carried out in Section 4. The conclusions of the study are presented in Section 5.

2.Literature review

The failure of the metal-patch interface has been investigated in the literature through experiments along with finite element simulations. Many researchers appropriately used FEM to simulate the interface separation; the noteworthy contributions being from Chau and Lee in 1998 [15], Tsamasphyros et al. in 2001 [16], Achour et al. in 2003 [17], Belhouari et al. in 2004 [18], Sekine et al. in 2005 [19], Haftchenari et al. in 2007 [20], Beukers et al. in 2007 [21], Ricci et al. in 2011 [22]. Bouiadjra et al. [23] carried out experiments on the repair of aluminium specimens having semi-circular notch, first with carbon/epoxy composite patch and then with fastened metal patch. The numerical simulations under the static and fatigue conditions were also performed. The composite patch was found to be superior in comparison to the metallic patch in terms of stiffness, weight, fabrication procedure, formability, mechanical properties and the cost. The study covered several aspects affecting the performance of the composite patching. Though the results were validated through experiments and simulations, the debonding mechanism was not addressed in this study. Shinde et al. [24] carried out a detailed experimental investigation of the crack repair using composite patch in aluminium specimens under tensile load. The monitoring factor considered was J-integral at the crack tip. The fiber reinforced patch was adept in arresting the growth of the crack till the load was below the yield stress of the parent metal. Beyond this point, the patch was rapidly separated resulting in a sudden failure. It was observed that full-width patches are not necessary as patches adequately covering the crack are equally effective. This study stated important aspects related to the failure process of the patch by incorporating J integral near the crack tip. But the study was limited as it only monitored parameters in a region near the crack tip. Grave and Echtermeyer [25] experimentally investigated non-linear behaviour of an adhesive joint of unidirectional carbon-epoxy composite patch through a strain field study; validated by FEM. The strain concentration near the crack tip increased due to non-linear effects. The design of the patch and prediction of the joint strength becomes challenging due to these non-linearities. The study included the non-linear effects during the patch failure process but it was based only on the strain field analysis. Benyahia et al. [26] compared the older and newer composite repairs. For a period of 120 days, the bonded composite patch specimen was dipped in water for accelerated aging and then its performance was evaluated in terms of change in the SIF. Through experiments on newer specimens, the structure's life was found improved when patch was used. There is a tendency of humidity absorption in case of the aged specimen which increases the SIF at the crack tip. Though the study provided important insights on accelerated aging conditions, the analysis was based on the SIF which accounts only for the crack tip behaviour. Beloufa et al. [27] used a three-dimensional FEM with contour integral to determine the SIF for mode I as well as combined mode I and mode II conditions in composite repair of cracks in aluminium panels. The patch strength was observed in direct proportion to the location of beginning of crack growth. The failure of the structure was found to be governed by distribution of stresses in adhesive. The arrangement of stacking of fiber layers in the patch decides the regions of critical stresses developed in adhered joint, patch and the metal panels. This study provided important conclusions on different factors but its limitation lies in the use of SIF as a basis of performance. Reburn [28] studied the behaviour of shear stress in a single lap joint between aluminium and glass fiber composite on the basis of fabrication parameters such as preparation of surface, process of bonding and the thickness of adherents. The maximum tangential stresses and normal stresses get developed in overlapping regions because of bending, caused by tensile load. A highly efficient co-curing process helps in controlling various factors during patch fabrication. The study elaborated on important patch fabrication parameters and also on the acting stresses during the loading. But it did not explain the exact process of interface separation. Ribeiro et al. [29] used computational techniques for analysing the single and double lap joints formed at the interface of metal and carbon-epoxy composite patch. It was concluded that a thicker adhesive leads to reduction in the stresses developed at the edge of the adhesive leading to an increase in the joint strength. A flexible adhesive helps in reducing the peak stress at the edge of the adhesive layer but its strength is low. As a shorter overlap length

leads to increased stress at the adhesive edge, a longer overlap is desirable but it can result in increased weight. An appropriate balance among various factors was recommended. The study was important from the selection point of view of the patch overlap length but it focussed on the stress analysis at the patch edges only. Vishnuvardhan et al. [30] employed FEM based algorithms for analysing the composite repaired aluminium plate having an edge crack in terms SIF. The major factors affecting the change in SIF were found to be the thickness of patch, its shape and the thermal loading conditions. Among the circular, rectangular and octagonal patch shapes, the rectangular patch was found effective in reducing the SIF. Though SIF decreased with increase in patch thickness, the reduction in SIF was small beyond a certain thickness of the patch. Since only SIF was considered as a factor in this study, it provided limited insights on the relation of repair performance with patch geometry. Ungureanu et al. [31] reviewed the theories of adhesion for polymer composite materials. The mechanical theory emphasizes on porosity and roughness of the contacting materials for a better adhesion as well as rheological characteristics of the adhesive. According to electrostatic theory, the electric discharge between adhesive and the parent material produces the adhesion effect. The surface forces between the contacting materials are responsible for causing adhesion as per the thermodynamic theory whereas the chemical bonding theory is based on adhesion due to chemical interactions. In actual practice, adhesive bonding is due to simultaneous effects of different theories. The study elaborated on the technical aspects of the adhesion, helping to understand appropriate conditions for composite patching but some of the practical aspects were not covered. Turan and Örçen [32] investigated the failure behaviour for different shapes of the notch (U-shape, V-shape, square-shape) for composite adhered plates through finite element simulation. The load to failure for a double-patch repair was greater than the failure load of the single-patch repair. The patch stacking sequence did not significantly affect the failure loads. The failure loads changed with the type of notch for a single sided repair but not for two-sided repair. The study seemed inadequate as the analyses of the substrate, adhesive and the patch were carried out separately. Ramakrishna et al. [33] compared the performance of carbon fiber composite patch repair for symmetric and asymmetric patches using FEM on the basis of stresses developed at the crack tip. The symmetric patches were found to be more effective than the asymmetric one in reducing the SIF. A better strength of the patch was observed in symmetric patches as compared to asymmetric patches. The study elaborated on the benefits of using symmetric patches but the complexities involved in the asymmetric repair were not addressed. Shinde et al. [34] investigated behaviour of aluminium specimens patched with carbon fiber composite on one side and subjected to uniaxial tension load. The number of layers of the patch were varied from one to three. It was found that the patch is separated from the surface when developed stress exceeds yield stress of parent metal, wherein the shear stress at the contact interface increases rapidly after exceeding the yield stress. The computational study was also carried out by employing the FEM using Ansys program. The study concluded that the repaired sheet should be bonded with an appropriately designed patch so that the adherent metal is loaded up to its yield stress. This study helped to understand various aspects of asymmetric patch repair but the exact process by which the failure of the patch occurs was not studied. A detailed review by Budhe et al. [35] on different aspects of adhesive bonding of composite patch to the metal revealed the importance of removal of surface contaminants during surface preparation so as to improve its wettability. The important parameters affecting the repair process were identified as thickness & width of adherent materials, thickness of adhesive and size of the patch. These parameters should be optimized for providing maximum strength to the joint. The analytical techniques fail to include material non-linearity, geometrical factors & contact interface. Also, experimentation is a costly & time-consuming affair. Therefore, it becomes imperative to employ computational tools such as FEM for studying the composite patching process. Echer et al. [36] employed computational tools for better understanding of effects of rectangular and elliptical patch shapes on composite repair process. The study was carried out for different stacking sequences of the patch layers. The results of the optimization study showed that rectangular and elliptical shapes are quite effective in arresting the crack growth despite their simple geometry. Aityala et al. [37] carried out numerical simulations of the composite repair process and identified the important parameters affecting the repair performance as elastic modulus of patch, shear modulus of adhesive and thicknesses of the patch & adhesive materials. The study was based on determination of SIF. The minimum value of SIF was obtained when adhesive shear modulus was high, elastic modulus of patch was high, patch thickness was small and adhesive thickness was high. The factor that largely affects the repair performance was identified

as adhesive shear modulus, whereas the other factors had a relatively small effect in the decreasing order of adhesive thickness, elastic modulus of patch and its thickness. The study provided an insight into important parameters affecting repair performance based solely on SIF near crack. The behaviour of contacting surfaces in areas other than crack tip was not studied. Özer [38] studied the basic properties of the adhesively bonded joint between similar and dissimilar materials. The advantages of using adhesive bonding in crack repair were notified as uniform stress distribution, decreased stress concentration, low cost, low weight, elimination of holes etc. The major parameters of performance were specified as type of joint, overlap length of the joint, material properties & thickness. A major challenge involved in adopting this method is to decrease concentration of stresses and maximizing the load to failure. In a single lap joint subjected to axial loads, a bending moment is developed due to load eccentricity which further develops interfacial stresses that become maximum at the ends of the overlap length. The study helped to understand the important consideration of maximizing the failure load for an effective performance of the composite patch. Fernandes and Campilho [39] emphasized the importance of using a CZM model in analysing the bonded joints in comparison to the other methods. The simple stress/strain approach is based on simplified assumptions, in which the obtained results may deviate from the actual results. The analytical methods do not address the inherent non-linearities present in the adhesive bonding process. The CZM model works on principles of fracture mechanics, which makes it relatively easy to model the initiation and growth of the crack. The authors performed numerical studies of adhesive bonding using bilinear, trapezoidal and exponential cohesive laws and found that the bilinear law is the most effective in studying the failure of adhesive bonds. The study covered the comparison of various models for analysing the adhesive bonding process. It accentuated merits of CZM and an appropriateness of cohesive law for an effective analysis of the composite patch repair process. Aabid et al. [40] carried out FEM in mode I condition to scrutinize the consequence of change in thickness of adhesive and patch along with length of the patch. The SIF was used as a criterion of evaluation which restricts the investigation in the vicinity of crack only. The SIF reduced when the adhesive thickness was reduced. Li et al. [41] carried out tensile tests on the adhesively bonded oblique square patched specimen and then the numerical simulation for understanding performance of the patch. The damage was caused majorly by fracture of fibers as revealed in X-ray tests. The study could not provide insights on the failure mechanism. El-sagheer et al. [42] studied the effect of bonding of glass fiber composite patch on an inclined crack in aluminium sheet with the help of three-dimensional FEM using different stacking sequences. The authors observed that the effectiveness of the patch depends on orientation of fibers with respect to the loading direction. A high stiffness of the patch is observed in parallel direction and the patch is more effective for mode-I condition. Bonding the patch on both sides of the crack is more effective but practically only one side of the crack is available for bonding in the majority of the applications. The study focussed on symmetrical patch repair under mode-I loading conditions but the detailed process of patch failure was not understood. Garg et al. [43] employed scaled boundary FEM for two-dimensional delamination analysis of composite laminates using bilinear CZM. The authors studied the behaviour of the patch under the conditions of mode I, mode II and combined loading. The results obtained in simulation studies were weighted against those available in literature for experimental work and the usefulness of scaled boundary FEM was underlined. Garg et al. [44] used the CZM technique to simulate two-dimensional composite laminates for delamination analysis under mode I, mode II and combined mode conditions. The interfacial cohesive elements were used at the contact surface under bilinear traction-separation law. The cohesive elements were assumed to be of zero thickness. The simulations were performed for different test conditions such as combined mode bending, flexure with end notch, double cantilever beam and combined mode with fixed ratio. A CZM model was found more effective than virtual crack closure technique and extended FEM. The comparison of various approaches to patch failure analysis was carried out in this study under different test conditions but the study of actual separation under working conditions was not made. Yousefi et al. [45] concluded through simulation study on SIF that stiffness and thickness of patch along with thickness of adhesive influences SIF. With the increase in volume fraction, there is an increase in various moduli such as in plane shear, out-of-plane shear, transitive and longitudinal moduli.

De and Donadon [46] presented a discussion on CZM behaviour to correlate energy dissipated, strength of patch and deterioration at the interface in terms of softening function which depends on the selection of loading and unloading curves. Appropriately selected curves result in residual strength in proportion with dissipated energy. A linear curve during loading and

unloading demands a similar nature of softening function. Wciślik and Pała [47] studied various aspects of the CZM model when used in the investigation of initiation and propagation of failure. The stresses, displacements and energy needed for creating a new surface are integrated in the cohesive model. The cohesive surfaces are placed in the plane in which the crack is expected to grow. The CZM model provides a versatile technique for solving a number of engineering problems for a variety of materials. The parameters required in CZM can be easily determined through experiments and numerical simulations. The issues of concern for CZM are its response to mixed mode loading, triaxial stress state and cyclical loading. The study was important from the point of view of understanding the importance of the CZM model. Echer et al. [48] conducted a comparative study on better shapes out of rectangular and elliptical patches in one-sided composite repair using FEM. These two shapes proved efficient in appropriately patching the cracked region despite their simple shapes wherein only two variables need consideration during design. The laying sequence of fibers layers also has an influence in determining the optimum shape of patch. The fibers are required to be perpendicular to the length of crack for improved repair efficiency. The study focussed on an important aspect of shape of the patch for an effective crack repair. Amari and Berrahou [49] probed into the influence of patch shape on the crack repair process through simulations using SIF and also through laboratory experiments. It was found that the maximum stresses occur at the tip of the crack and they grow as the crack propagates further. The total patch was found effective in arresting the crack as compared to U-shape of the patch. The limitation of the study was in determining the ultimate strength of the patched specimen rather than determining the failure stress. Benkheira et al. [50] carried out experimental and numerical work to probe into different factors influencing composite patching such as length of patch, width of patch, properties of adhesive, single-side / two-side repair and method of repair. The derived conclusion suggested that efficiency of patch relies on adhesive properties, patch length and zone of deboning in the adhesive layer. Though the experimental and numerical results matched with a convergence ratio of 5 to 10%, the number of elements in the numerical analysis were limited. For improving simulation results, element sizes can be reduced to further finer limits. Berrahou and Amari [51] conducted FEM of the repair in three dimensions made by using boron/epoxy, graphite/epoxy and glass/epoxy composite materials with different shapes. The investigation was based on SIF and stress distribution. The results showed that the boron/epoxy material was the most efficient in arresting the growth of the damage. The optimum performance was obtained when the shape of the patch covered the total damage area. As the study was based on the SIF, it focussed mainly on the stresses at tip of the crack and ignored stresses in other regions such as ends of the patch. Tamboli et al. [52] carried out the study of composite patch repair with carbon fiber composite for an inclined crack in aluminium sheet through experiments under fatigue loading. The ply drop technique was employed in which the successive plies are reduced in length for multilayered patches. The ply-drop was found effective for reinstating the original strength of structure. This study accentuated the role of interfacial shear stress rather than fracture toughness parameters. The combined effect of different stresses was not considered in this study. Aabid et al. [53] carried out a numerical study to find a two-sided optimum patch on the basis of mode-I SIF in the repair of center crack in an aluminium sheet. Taguchi method was incorporated for optimising the defined parameters using a L9 orthogonal array. The parameters considered for optimization study included thickness of patch, adhesive thickness and cross-sectional patch area. Optimum parameters were obtained by employing design of experiments and analysis of variance. The study of optimisation of important parameters in composite repair can help in designing an appropriate patch. Shinde et al. [54] made an investigation into fatigue life prediction of a thin pre-cracked aluminium sheet adhered with a composite patch on one side of the specimen using numerical technique with the help of CZM and SIF. The study concluded that the SIF reduces with the increased patch length, thus leading to increased fatigue life. The limitation of the study lies in the study being concentrated at crack-tip SIF. Khode and Nimje [55] performed FEM in three dimensions of composite patch repair adhered with a central circular patch. The stress concentration at critical regions of the adhesively bonded joint was reduced by using functionally graded adhesive material. Higher modulus ratio is desirable as it causes uniform stress distribution in the bond region. This study was based on the out of plane stresses assuming that only these stresses are responsible for debonding of the patch. But in practice it is the combined effect of different types of stresses which causes the debonding. Abdelfattah et al. [56] carried out the experimental and numerical studies of three-point bend analysis of the patch repair with square shaped single-sided carbon polymer patch. The efficiency of the patch repair was studied on the basis of various parameters i.e. bondline

shear and normal stresses, flexural moduli, and load at ultimate point. Though this investigation could predict optimum conditions for one-side patch, the major emphasis was weighted on flexural conditions. Luo and Liang [57] performed a study with the help of experiments and also using computer simulations on repair of aluminium alloys sheet using carbon fiber reinforced patches. The extended finite element analysis and traction-separation law were employed for this study. The study confirmed enhanced efficiency of composite patching in crack repairing; tensile strength being the criterion of evaluation. An emphasis on usage of traction-separation law in simulation of patch failure was stated.

Thus, the study of the composite patch repair has been carried out by different researchers as noted in the available literature using experimental methods, analytical techniques and also through computational techniques. It was found that the experiments provide only the values of loads at different instances. On the other hand, there are simplified assumptions in analytical techniques which exclude nonlinearities. The FEM has proved as an effective technique for understanding the performance of the patch repair. The CZM has also been incorporated in the modern commercial FEM software which helps in simulating the failure process. Though composite repair techniques have been used extensively in industry, the exact mechanism by which the patch separates from its substrate is still not fully known. As a number of factors are involved in the separation analysis, it increases the complexity of the analysis. An attempt is made in this research to understand the patch separation process using a combination of the experiments and numerical method.

3.Methods

The study was carried out by using experimental and numerical methods. The patched specimens were subjected to loading in the experiments to determine the failure stresses. The simulations of experiments were conducted through FEM. Results obtained in both methods were compared and reliability of finite element simulation was confirmed. The process of failure of patch was then studied by analysing nodal stresses, displacements, energies and separated areas obtained through FEM.

3.1Experimental method

The experimental method included the preparation of a specimen having a center crack and then repairing the crack by adhering fiber reinforced composite patch on the cracked region using vacuum bagging technique. The length of the specimen was 400 mm, width was 60 mm and thickness was 1 mm. The specimen was cut from an aluminium sheet having rolling direction along its length and a 25 mm long crack was cut in it. Glass-fiber-reinforced-polymer (GFRP) layer of composite patch was prepared by impregnating glass-fiber reinforcement into epoxy-resin. Similarly, carbon-fiber-reinforced-polymer (CFRP) layer of composite patch was prepared by impregnating carbon-fiber reinforcement into epoxy-resin. At the cracked location, the two layers of the patch were adhered; a separating first layer of 76 gsm of unidirectional glass-fiber (modulus of elasticity = 85.5 GPa) of 70 mm length (L) and a load bearing second layer of 160 gsm of unidirectional carbon-fiber (modulus of elasticity = 230 GPa) of 50 mm length. Both GFRP and CFRP layers were made of equal width (W) of 36 mm. Epoxy, the thermosetting resin [Dobeckot 520F manufactured by Elantas Beck India Ltd (100 parts by weight) with hardener 758 (9 parts by weight) with modulus of elasticity = 3 GPa] was used as matrix material in both patch layers. The epoxy acts as a binding agent for adhering the patch to the metal substrate. 0.5% by weight 3-aminopropyltriethoxysilane was also used as an adhesion promoter which improves the chemical bonding of resin with the reinforcement. The patch was adhered only on one side of the cracked specimen since both sides are not generally accessible in practical applications. The specimen was kept in a vacuum bag consisting of teflon sheet, perforated sheet, breather, bagging sheet and vacuum port. A pressure of 600 mm of Hg vacuum was maintained inside the vacuum bag with the help of a vacuum pump for 4 hours. After this, the specimen was cured in air under dead-weights for more than 24 hours followed by post-curing for 5 hours at 80 degree celsius in an oven. In *Figure 1*, the prepared specimen is exhibited in which the crack edge is an edge at crack location while leading edge is an edge at the end of patch.

The specimen was then subjected to uniaxial tensile load on a universal testing machine of 10-ton capacity. The cross-head of the machine could be run at a speed of 0.1 mm per min under normal temperature and humidity conditions. Tapered blocks were used as grips along with a stiff die for holding the specimen in the cross-head during tensile tests. One end of the specimen was fixed by clamping while its free end was uniformly displaced (u1), ensuring that uniaxial tensile load could act on the specimen. With increasing displacement, the tensile load was gradually increased which induced stresses in the metal panel. The stresses were also induced at the contact surface between the

metal panel and patch. Stresses were also induced in the composite patch. These increasing stresses caused the patch to slip when the threshold value was exceeded; initiating separation of patch from the metal panel. As the applied load was increased to higher values, the separation rate became very high and finally the patch was completely separated from the aluminium specimen. The load to failure and its location were recorded in the experimental procedure. Once the patch was separated, there was a transfer of load from patch to crack causing it to grow rapidly and resulting in complete breakage of the specimen.

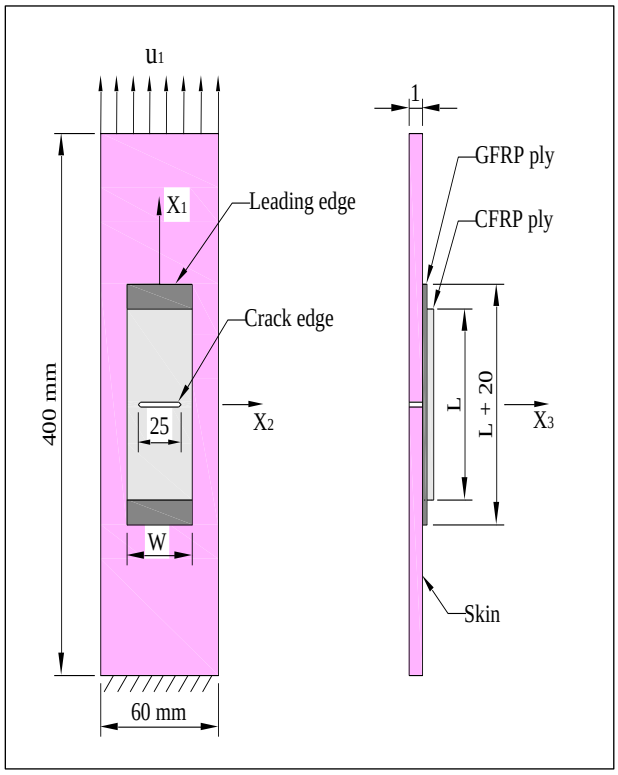

Figure 1 Patched specimen

3.2Numerical method

Understanding the nature of separation that occurs at the contact surface is essential as it can help in identifying parameters that affect the failure process and also in redesigning the patch to increase its effectiveness. The physical experiments help only in determining the failure load & its location. For understanding the failure mechanism which involves an analysis at the contact surfaces, the knowledge of the state of the stresses at different instances is needed. The FEM makes such an analysis possible. The FEM analysis was conducted in Ansys software. Patched specimen was modelled in the design modeller module of Ansys followed by its meshing. SOLID186 elements were used for meshing aluminium panel and the layers of composite patch. SOLID 186 follows a quadratic type of displacement falling in the category of higher order element having 20 nodes. An optimum size of mesh along width direction was arrived at by performing a convergence study by varying it in the range between 1.28 mm to 0.16 mm by successively reducing it to half (1.28, 0.64, 0.32 and 0.16 mm).

Numerical analyses were performed with these mesh sizes and the output results were compared. A negligible difference of less than 3% in output results was observed for mesh sizes of 0.16, 0.32 and 0.64 mm. Based on this, it was decided to consider 0.64 mm as the optimum size for width direction as reducing mesh below this doesn't give any additional advantage. Similar convergence studies were conducted in length as well as thickness directions. It was ensured that the elements near the crack and leading edges remained of small sizes (0.13 mm) as these were the areas of stress concentration. A large size of mesh was used at farther locations. The mesh of the aluminium panel had 4 elements (0.25 mm mesh size) in the thickness direction. The glass fiber and carbon fiber layers had only one element in their mesh in thickness direction with sizes of 0.12 and 0.22 mm respectively. It was ensured that the nodes at the contacting surfaces were coincident. Instead of the full model, only one-forth of the model was analysed as it reduces the requirements of computational resources. *Figure 2* exhibits the quarter model of the specimen. On the planes O-R and O-M, symmetric boundary conditions were employed. O-T is the plane of the crack acting as a free surface. The free-end R-N of the quarter model was subjected to a gradual and uniformly increasing displacement in a direction in which the loads were acting.

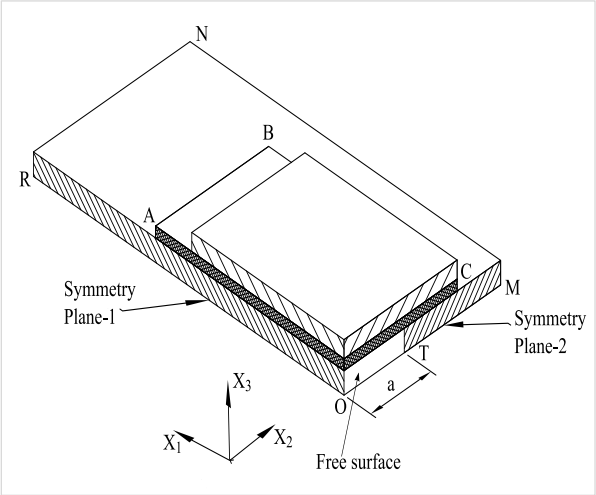

Figure 2 Boundary conditions on quarter model

Since the analysis involves the failure at the interface of two different materials, a special set of three-dimensional quadratic element INTER204 incorporating a CZM model was used at the metal-patch interface. A tensile load was applied on the finite element model perpendicular to the crack length. The same is shown in *Figure 3*.

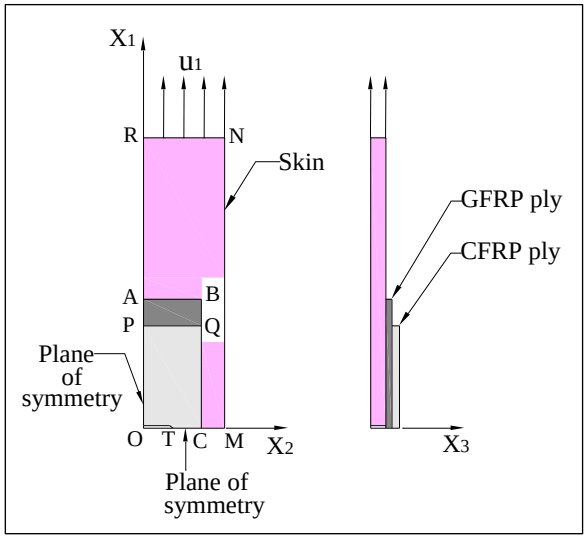

Figure 3 One-fourth model of specimen

The CZM does not represent any physical condition but corresponds to cohesion forces at the interface and accommodates the separation. In fact, there exists a small zone named as cohesive zone at the tip of the crack wherein the gradual separation occurs. The CZM model is characterized by separating nodes located in a cohesive zone as the two contacting materials separate at their interface. The cohesive zone captures behaviour at the contact surface, representing a variation in its traction with changing displacement at different nodes. It is known that the complex phenomenon of interface failure is a result of simultaneous existence of the traction in normal and tangential directions [58, 59]. This causes the failure to occur in a mixed mode; failure in mode-I due to the stresses in normal direction causing a peeling action and failure in mode-II due to the stresses in tangential direction producing a shearing action. The most commonly used bilinear model was employed in which the traction and displacement follows a linear relationship during increasing and decreasing state of the tractions as per the traction-separation law in normal & tangential directions as shown in *Figure 4* [59, 60]. There is a linear increase in traction with increase in displacement that reaches its maximum value followed by its linear decrease until the displacement becomes zero, thus leading to a complete separation. The area corresponding to the maximum traction gives the critical fracture energy which when exceeded causes the complete failure.

The traction-separation law helps to express the failure process in terms of energy variation; termed as energy release rate; which corresponds to the amount of energy required to separate two bonded surfaces. The normal yield stress of the epoxy matrix, T_n^{max} = 35 MPa was considered as the maximum normal traction whereas the tangential yield stress of the epoxy matrix, T_t^{max} = 25 MPa was considered as the maximum shear traction. Area under curve O-A-C represents an energy which produces separation in mode I. This energy was named as critical energy release rate i.e. critical fracture energy (G_{Ic}) given by Equation 1.

$$G_{Ic} = \frac{1}{2}(T_n^{max}) \times (\delta_n^c) \quad (1)$$

where δ_n^c is the separation in normal direction at the completion of debonding. G_{Ic} was evaluated through a separate in-house experiment as $52 \pm 29 J/m^2$. From the values corresponding to G_{Ic} and T_n^{max}, the mode I critical separation could be found out as 0.00297 mm. On the similar lines, an area O-A-C in *Figure 4* corresponds to critical energy release rate in mode-II (G_{IIc}) given by Equation 2.

$$G_{IIc} = \frac{1}{2}(T_t^{max}) \times (\delta_t^c) \quad (2)$$

where δ_t^c is the separation in tangential direction at the completion of debonding. G_{IIc} as 638 ± 74 J/m^2 and critical displacement δ_n^c as 0.051 mm were found out through a separate study.

The load induced in the aluminium panel was transferred to the patch at contact surface through a tangential (shear) stress of high value which was developed near patch edges i.e. crack and leading edges. The asymmetric nature of the one-side patch produced a bending effect and resulted in development of a normal (peel) stress of high value at the contact surface. The separation at the contact surface of the aluminium panel and the patch occurred because of the combined action of normal and tangential stresses. This led to employing a mixed-mode-criterion (MMC) of separation which consisted of a combination of mode I and mode II criteria. MMC was expressed by an energy criterion as per the power law given by the inequality shown in Equation 3.

$$\text{MMC} = \left(\frac{G_I}{G_{Ic}}\right)^2 + \left(\frac{G_{II}}{G_{IIc}}\right)^2 \geq 1 \quad (3)$$

where G_I and G_{II} represent instantaneous values of energy release rate in mode I and mode II respectively.

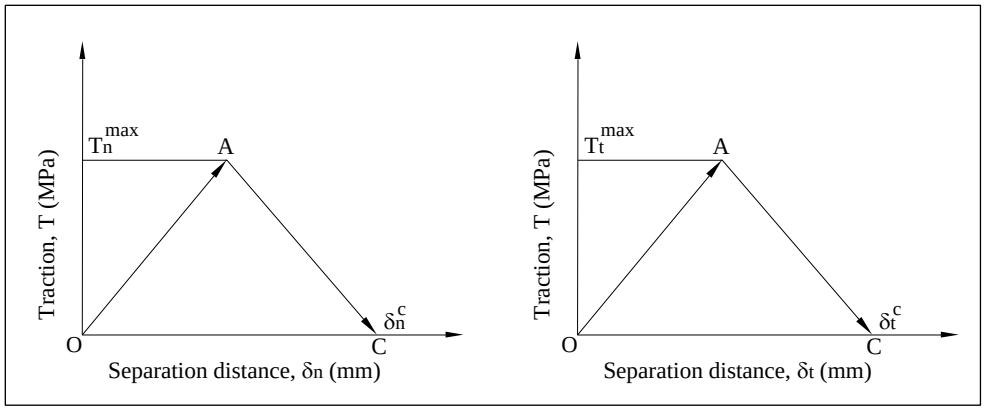

Figure 4 Bilinear model in normal and tangential directions

The instantaneous values of nodal stresses and displacements were determined through finite element simulations. Using these instantaneous values, the instantaneous energy release rate was determined which was then compared with the critical value of energy release rate and the state of failure was understood. The MMC criterion was applied at different nodes at various instances of loading. The node was considered to be separated when MMC was greater than 1. This approach helped to understand the state of separation at different nodes located in an area under consideration. A great number of equations are generated during finite element simulations which are simultaneously solved through in-core memory of software using sparse direct solver. The computer system used for these simulations was a workstation of advanced configuration employing Intel Xeon processor along with a RAM of 32 GB capacity and a ROM of 1.5 TB capacity. A high amount of storage memory, ranging from 4 GB to 15 GB was required on the hard disk. The finite element analysis was heavy on computational resources which lasted for several hours i.e. 18-24 hours depending on the number of elements. The nodal values of the stresses and displacements were extracted from the result files and the instantaneous variation in energy release rate and the separated area were determined at different instances. This procedure consumed a fair amount of time, thus increasing the total processing time.

4.Results and discussion

A number of experiments and simulations were performed with constant length - varying width and also with constant width - varying length of patch. Failure stresses from experiments and simulations were compared as presented in *Table 1*. The results derived from experiments matched well with the simulation results; the difference between the two being very small. The maximum difference of 7.1% was observed for the patch configuration of 20 mm length and 48 mm width. In fact, the difference was less than 2.6% for four experiments. The difference between the two kinds of the results can be accrued to the approximations during solving of the equations in finite element simulation. Since the results matched quite well with those in the experiments, the reliability of finite element simulations was confirmed.

Table 1 Comparison of experimental and simulation results for single-layered patch

Sr. no.	Patch dimensions		Failure stress		
	Length (mm)	Width (mm)	Experimental values (MPa)	Simulation values (MPa)	Difference (%)
1	50	30	302.0	294.3	2.6
2	50	36	319.8	327.0	2.3
3	50	42	327.0	338.6	3.6
4	20	48	272.6	292.1	7.1
5	25	48	295.3	292.3	1.0
6	30	48	297.6	292.5	1.7
7	40	48	313.6	332.8	6.1
8	45	48	318.3	338.6	6.4
9	50	48	320.8	338.7	5.6
10	70	48	337.2	338.9	0.5

4.1Initiation of separation

The behaviour of the patched specimen under the action of uniaxial tension load was studied through finite element simulations which is elaborated in this section. Considering the symmetrical nature of the specimen, only a quarter portion of the specimen was numerically simulated. With the increase in the uniaxial displacement at the free end of the specimen, axial stresses (σ) were induced in the specimen. These induced stresses were shared by the metal sheet and the patch and were transferred from metal to the patch through the contact interface. *Figure 5* exhibits the two types of stress components developed at the interface; peel stress (σ_{33}) and shear stress (σ_{13}). An axial stress in aluminium was transferred through shear stress (σ_{13}) into the patch. Since the patch was applied on a single side of the specimen, this asymmetry causes a bending effect and develops a peel stress (σ_{33}) acting in a direction normal to the interface.

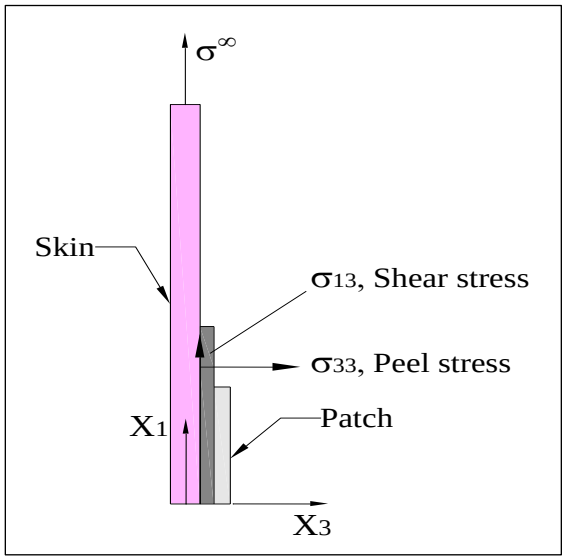

Figure 5 Stress components at contact surface

Figure 6 exhibits the specimen and induced stresses at the applied stress of 147 MPa at which the separation of the patch from the metal surface was about to initiate. The transfer of the stress from metal into the patch occurs through shear stress and can be visualized to be taking place from point R to O in *Figure 6(a, b);* first at a Leading Edge of glass fiber layer (LE, G) of the glass fiber layer and then at leading edge of carbon fiber layer (LE, C) of carbon fiber layer.

As seen in *Figure 6(c)*, the transfer of axial stress from metal into the patch created a small spike of shear stress (2.25 MPa) near LE, G, reducing the axial stress from 147 MPa to 127 MPa. A similar shear stress spike (2.74 MPa) was created near LE, C, reducing the axial stress further to 102 MPa. The change in axial stress is depicted in *Figure 6(d).*

The leftover stress was transferred to the patch at point 'O' (crack edge) through shear, creating a spike of 10.45 MPa. During this transfer, the peel stress also varies as shown in *Figure 6(e).* Small spikes of peel stress of 0.43 MPa and 5.8 MPa were observed at the edges of glass fiber and carbon fiber layers respectively. A large spike of 31.08 MPa was created in the crack region due to bending action produced because of the asymmetric nature of the patch. Thus the shear stress (σ_{13}= 10.45 MPa) and the peel stress (σ_{33}= 31.08 MPa) were maximum at the crack edge OT. This combined effect of the loading i.e. mode-I by peel stress and mode-II by shear stress resulted in initiation of patch separation. The MMC was incorporated at different nodes for which the instantaneous values of energy release rate G_I & G_{II} were determined as per the bilinear traction-separation law.

The crack edge was the location at which the separation of patch began when the applied stress was between σ^{∞}=142.8 MPa to 147 MPa. At σ^{∞}=142.8 MPa, G_I and G_{II} were determined at a node located at the crack center using the values of the stresses and corresponding nodal displacements. The values of the peel stresses and shear stresses were σ_{33}= 31.08 MPa and σ_{13}= 10.45 MPa which helped to determine the values of energies i.e. G_I = 39.5 J/m^2 and G_{II} = 113.6 J/m^2. The value of MMC was determined as 0.65 as per Equation 3 which was less than 1; thus, showing that the node was still not separated from the metal sheet. When the applied stress was 147 MPa, the shear and peel stresses became maximum and then suddenly dropped to zero. The values of G_I & G_{II} were determined as 60.4 J/m^2 & 122 J/m^2 respectively and the corresponding value of MMC was 1.49 (>1). Thus, the central node near the crack was separated from parent metal. The MMC was applied to a few nodes surrounding this central node and it was found that these nodes were also separated. Thus, the separation of the patch from the parent metal was initiated with a small area of separation.

4.2Growth of separation area

Once the separation began at point 'O' (crack center), the area of separation started to grow when applied stress exceeded 147 MPa. This growth of separated areas is depicted at different applied stresses in *Figure 7* by the shaded portion.

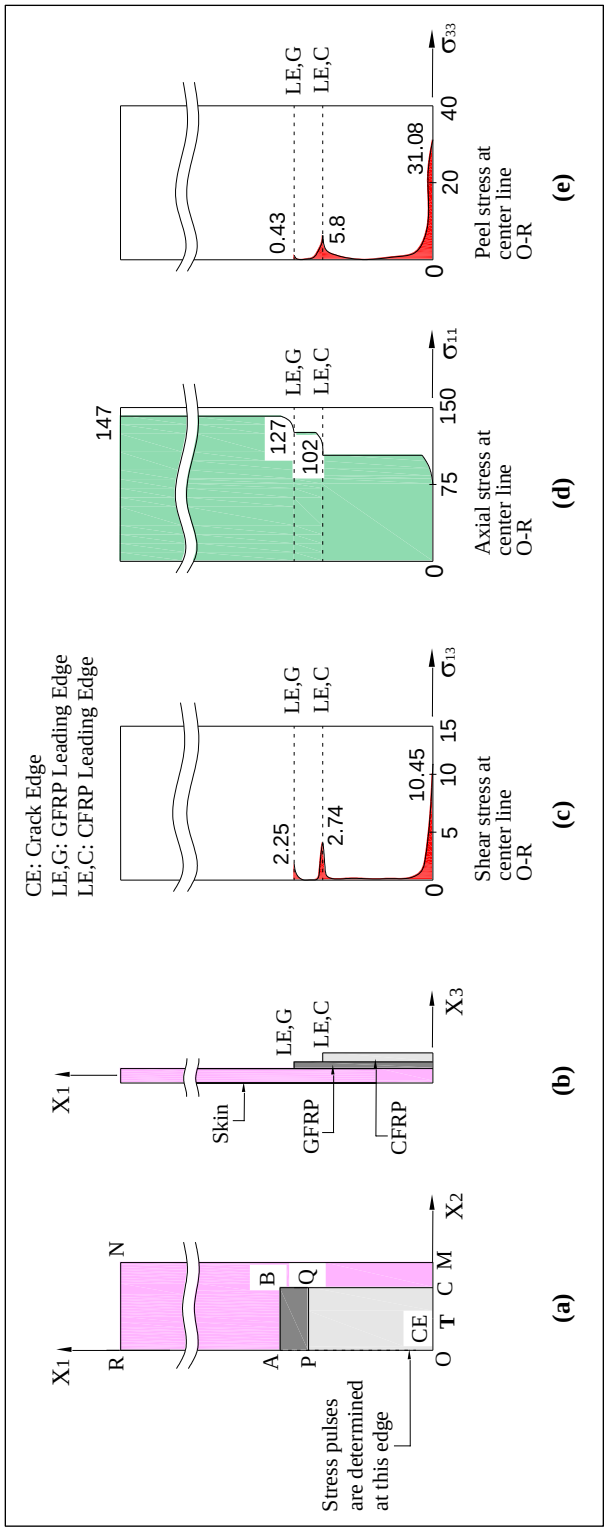

Figure 6 Quarter model of specimen showing; **(a)** front view, **(b)** side view, **(c)** interfacial shear stress (σ_{13}), **(d)** skin axial stress (σ_{11}), **(e)** interfacial peel stress (σ_{33}) at center line O-R at 147 MPa

The distribution of the shear stress is also exhibited in *Figure 8* and *Figure 9* at varying applied stresses. The separated area at an applied stress of 147 MPa was so small that it is practically not visible in the first sketch of *Figure 7* as very few nodes near the crack center were separated.

The second sketch of *Figure 7* shows the separated area at the applied stress of 235 MPa and *Figure 8* shows its shear stress distribution. The separated area at 235 MPa is represented by the region O-D-E consisting of completely separated nodes at which the shear stresses became zero. Just beyond D-E, high shear stress was observed as the adjacent nodes were only partially separated and the peel stress was also high. The mixed mode failure criterion was incorporated in this area. The values of energy release rate were determined as G_{II} = 13.5 J/m^2 and G_I = 0.019 J/m^2 at the glass fiber leading edge (point A) and the corresponding MMC was far less than 1 (MMC = 0.0004); indicating that the nodes were still not separated in this region. At point B on the glass fiber edge, the nodes remained adhered to the interface as MMC was 0.0005 with G_I = 0.023 J/m^2 and G_{II} = 14.6 J/m^2. The failure criterion was also verified at the edge of the carbon fiber layer (points P & Q) and the values of MMC, significantly less than the limiting value, were obtained as 0.003 and 0.007 respectively. Thus the nodes in the region containing the carbon fiber were also not separated. Thus at the applied stress of 235 MPa, the separation area grew in the crack region and there was no separation at the edges of the glass fiber and carbon fiber layers.

Beyond 235 MPa, the separated area at crack edge started growing at a steady rate with the nodes in that region getting separated progressively till the applied stress was 260 MPa. Once the stress increased above 260 MPa, there was rapid growth of separated areas from 260 MPa to 327 MPa. The same is exhibited in *Figure 9* which also depicts peak value of shear stress near separation front in each case wherein the peel stress was also high.

For all six cases of *Figure 7*, there was no separation at the edges of the glass fiber and carbon fiber layers as per the MMC failure criterion and the separation was observed only in the region of crack edge. Beyond the axial stress of 327 MPa, the simulation stopped because of the numerical instability caused by a large nodal displacement. This can be understood from the graphical relation shown in *Figure 10*, showing the variation of induced stress with the change in applied displacement. There was a linear increase in the

induced stress when the applied displacement was increased in the displacement control mode of loading. This linear increase was observed at a high rate till the induced stress was near 300 MPa; beyond which the rate of increase was lowered. The induced stress peaked at an applied displacement of 2.9 mm beyond which the induced stress began to decrease, creating a condition of numerical instability. This peak stress was considered as the failure stress.

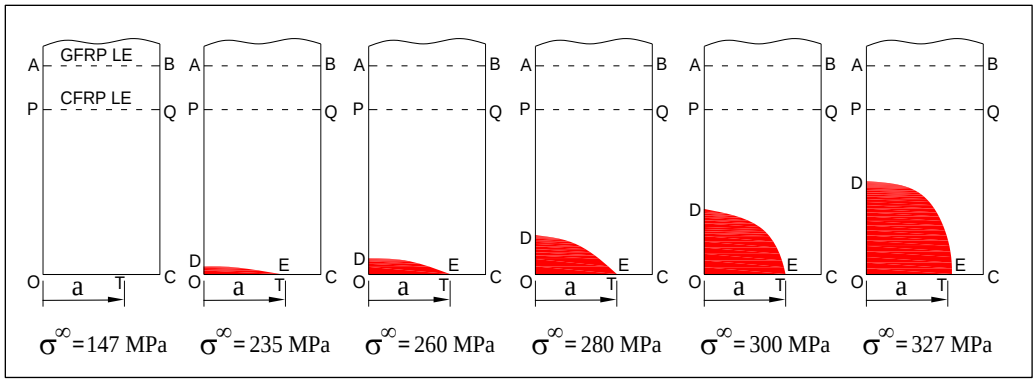

Figure 7 Growth of separation area

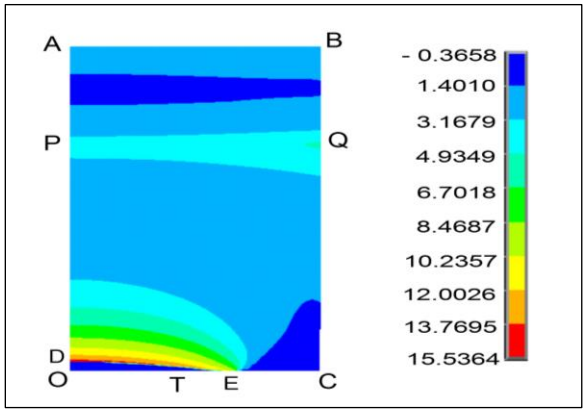

Figure 8 Distribution of shear stress at an applied stress of 235 MPa

Figure 11 shows the change in the separated area with change in the applied stress. The initial rate of increase of separated area was slow and steady till 280 MPa. The separation occurred at an elevated rate beyond yield stress of the metal sheet which continued at this high rate till the applied stress became greater than 327 MPa. At this point, a large patch area was separated along the length and width directions in the crack region; leading to complete patch failure. Thus, the patch failed due to its separation from the parent metal in the crack region and no separation occurred near the edges of the glass fiber and carbon fiber plies. The specimen failed by interface separation at an average failure stress of 319.8 MPa as measured in experiments. The difference between the values of the failure stress obtained in experimental work and through simulation was less than 3% which is considered not to be significant.

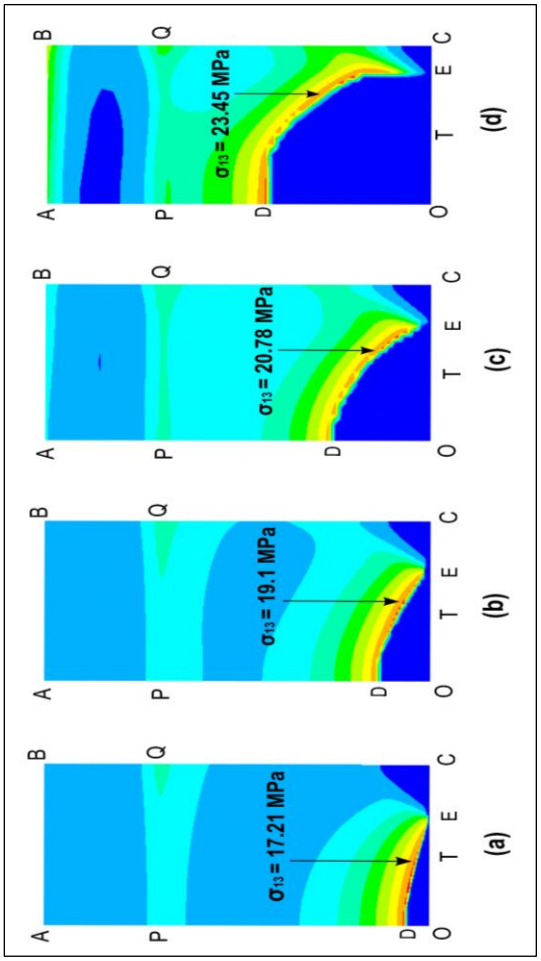

Figure 9 Growth of separation front through increasing shear stress (σ_{13}) at **(a)** 260 MPa, **(b)** 280 MPa, **(c)** 300 MPa and **(d)** 327 MPa

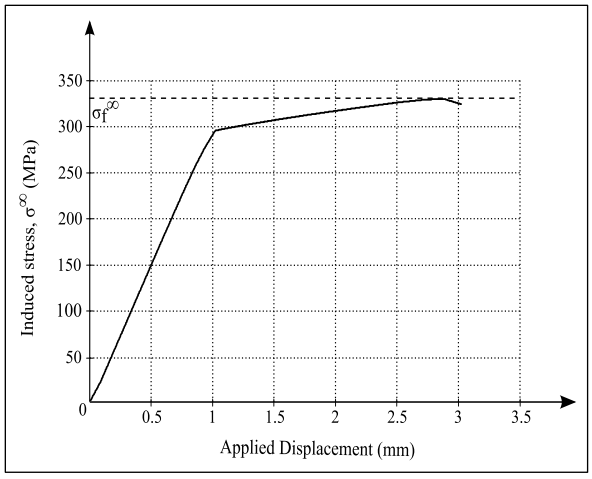

Figure 10 Variation of induced stress with applied displacement

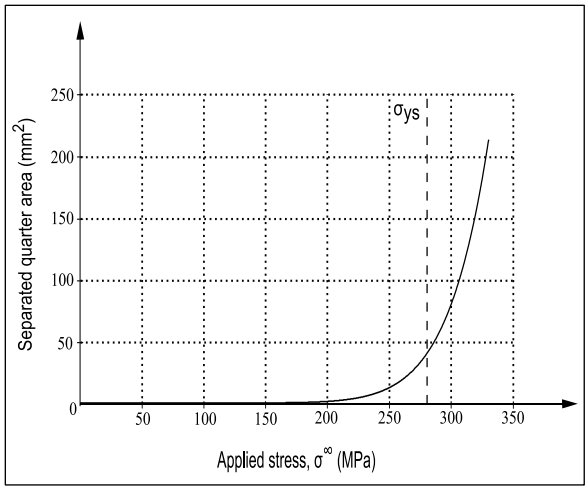

Figure 11 Separation curve

Thus, the mechanism of patch failure was understood using the numerical analysis and CZM model. Because of the applied loads, axial stresses are induced in the patched specimen which are transferred from the parent metal into the patch through their contact interface. The peel stress and shear stress at the contact surface produce peeling (mode I) and shearing (mode II) actions. These combined stresses cause the beginning of separation. This phenomenon could be understood through energy release rates at various nodes and the MMC value. The separation areas were determined by employing this method in the regions near the crack and patch edges. The stresses, displacements and energies were determined for the increasing applied stresses along with the separated areas. The rate of separation increased linearly until the applied load became equal to yield stress of metal. Beyond this yield stress, the rate of separation increased rapidly and at high value of the stress, the complete failure of patch occurred. With variation in patch length and width, a similar mechanism was observed; the only difference being the separation at the patch edges along with crack edge separation in some cases. For all experiments listed in *Table 1*, failure stress exceeds the yield stress of aluminium. Failure of patch for 50 mm length and small width (30 & 36 mm) was initiated at the edge of the crack followed by a rapid growth until its complete failure. For patches of 50 mm long and width greater than 42 mm, failure was initiated at the edge of the crack and later at the edge of the glass fiber layer; followed by a rapid growth of separated area till the complete patch was separated. With 48 mm patch width, the failure initiated at the edge of the crack and grew rapidly for smaller lengths of the patch (20 mm - 45 mm). With 48 mm width and longer patches (50 & 70 mm), the failure was initiated at two locations; initially at the crack edge and then at the edge of the glass fiber layer at higher applied stress. The rate of separation increased at a faster rate at higher stress and then finally the patch failed completely. Thus, the patch separation mechanism could be understood with the help of the advanced computational tools i.e. finite element analysis and CZM model. This understanding could help in redesigning the patch geometry for selecting an optimum patch configuration. The effect of the increase in the number of patch layers could also be understood through similar procedures. The future studies could include temperatures affecting performance of the composite repair. Future research could also be based on the effect of fatigue loading on the composite patch behaviour.

4.3Limitation of the study

The experimental procedure for understanding the patch failure process involves the breakage of the specimen under high values of loads. The preparation of the specimen is a tedious process involving multiple steps. Practically it was difficult to carry out experiments with various patch configurations because of the constraints on the funds and other resources. Therefore, the finite element simulations were conducted for various patch configurations which could not be validated experimentally. A complete list of abbreviations is listed in *Appendix I.*

5.Conclusion and future work

A pre-cracked aluminium metal specimen was adhered with a single layered carbon fiber composite patch having glass fiber ply as a separating layer. A model of patched specimen was analysed for understanding patch failure mechanism by employing

CZM. Stresses at contact surface and area of patch that was separated during loading were monitored. The energy release rates were determined from these parameters. The adhered patch separated at the contact interface because of the combined effect of normal and tangential stresses producing a mixed mode of failure. The patch began to separate in the crack region with an initial slow rate. The separation occurred at a high rate above the yield stress of the metal; with a large patch area getting separated from the parent metal and it failed completely at the failure stress. Thus, the complex mechanism of patch failure could be understood with the help of numerical simulation. The future work involves the finite element simulation for different configurations of the patch and also for patches with multiple layers. The optimization study could be performed for determining the optimum size and thickness of patch. The mechanism of patch failure under fatigue loading conditions can be studied with an approach similar to this study.

Acknowledgment
None.

Conflicts of interest
The authors have no conflicts of interest to declare.

Data availability
The data considered in this study were gathered during the doctoral research carried out at COEP Technological University. The data are not publicly available. However, the data may be provided by the corresponding author upon reasonable request.

Author's contribution statement
Amol Rasane: Conceptualization, investigation, data curation, writing – original draft, writing – review and editing. **Prashant Kumar:** Study conception, design, supervision, investigation on challenges and analysis and interpretation of results. **Mohan Khond:** Supervision, investigation on challenges and analysis and interpretation of results.

References
[1] Ratwani MM. Repair options for airframes. Aging Aircraft Fleets-Structural and Other Subsystem Aspects. 2000.
[2] Marazani T, Madyira DM, Akinlabi ET. Repair of cracks in metals: a review. Procedia Manufacturing. 2017; 8:673-9.
[3] Baker A. Bonded repair of aircraft structures. Springer Science & Business Media; 1988.
[4] Baker AA, Rose LF, Jones R. Advances in the bonded composite repair of metallic aircraft structure. Elsevier; 2003.
[5] Duong CN, Wang CH. Composite repair: theory and design. Elsevier; 2010.
[6] Sun CT, Klug J, Arendt C. Analysis of cracked aluminum plates repaired with bonded composite patches. AIAA Journal. 1996; 34(2):369-74.
[7] Rastogi N, Soni S, Denney J. Analysis of bonded composite patch repaired metallic structures-an overview. In 39th AIAA/ASME/ASCE/AHS/ASC structures, structural dynamics, and materials conference and exhibit 1998.
[8] Colombi P, Bassetti A, Nussbaumer A. Delamination effects on cracked steel members reinforced by prestressed composite patch. Theoretical and Applied Fracture Mechanics. 2003; 39(1):61-71.
[9] Okafor AC, Singh N, Enemuoh UE, Rao SV. Design, analysis and performance of adhesively bonded composite patch repair of cracked aluminum aircraft panels. Composite Structures. 2005; 71(2):258-70.
[10] Davis MJ, Janardhana M, Wherrett A. Adhesive bonded repair technology: supporting aging aircraft. In Ageing Aircraft Users Forum, Brisbane. 2006.
[11] Liu HB, Xiao ZG, Zhao XL, Al-mahaidi R. Fracture mechanics analysis of cracked steel plates repaired with composite sheets. In Asia-Pacific conference on FRP in structures, Hong Kong, China 2007 (pp. 1047-52).
[12] Kwon YW, Lee WY. Analytical model for single-side patch design of composite repair. Monterey, California: Naval Postgraduate School; 2013.
[13] Khan SM, Essaheb M. Effect of patch thickness on the repair performance of bonded composite repair in cracked aluminum plate. Materials Today: Proceedings. 2017; 4(8):9020-8.
[14] Ramji M, Srilakshmi R. Design of composite patch reinforcement applied to mixed-mode cracked panel using finite element analysis. Journal of Reinforced Plastics and Composites. 2012; 31(9):585-95.
[15] Chau RW, Lee SW. Computational modeling and analysis of a center-cracked panel repaired by bonded composite patch. Key Engineering Materials (Switzerland). 1998; 145(1):601-6.
[16] Tsamasphyros GJ, Kanderakis GN, Karalekas D, Rapti D, Gdoutos EE, Zacharopoulos D, et al. Study of composite patch repair by analytical and numerical methods. Fatigue & Fracture of Engineering Materials & Structures. 2001; 24(10):631-6.
[17] Achour T, Bouiadjra BB, Serier B. Numerical analysis of the performances of the bonded composite patch for reducing stress concentration and repairing cracks at notch. Computational Materials Science. 2003; 28(1):41-8.
[18] Belhouari M, Bouiadjra BB, Megueni A, Kaddouri K. Comparison of double and single bonded repairs to symmetric composite structures: a numerical analysis. Composite Structures. 2004; 65(1):47-53.
[19] Sekine H, Yan B, Yasuho T. Numerical simulation study of fatigue crack growth behavior of cracked aluminum panels repaired with a FRP composite patch using combined BEM/FEM. Engineering Fracture Mechanics. 2005; 72(16):2549-63.
[20] Haftchenari H, Varvani-farahani A, Jahandardost M. Stress intensity factors in un-repaired and repaired cracked aluminum panels by CFRP composite patch-

FE analysis. In 48th AIAA/ASME/ASCE/AHS/ASC structures, structural dynamics, and materials conference 2007. ARC.
[21] Beukers A, Koussios S, Boer HJ. Modeling Interfaces and bonded joints. In 16th international conference on composite materials 2007 (pp. 1-9). Japan Society for Composite Materials.
[22] Ricci F, Franco F, Montefusco N. Bonded composite patch repairs on cracked aluminum plates: theory, modeling and experiments. Advances in Composite Materials-Ecodesign and Analysis. 2011; 20:445-64.
[23] Bouiadjra BB, Benyahia F, Albedah A, Bouiadjra BA, Khan SM. Comparison between composite and metallic patches for repairing aircraft structures of aluminum alloy 7075 T6. International Journal of Fatigue. 2015; 80:128-35.
[24] Shinde PS, Kumar P, Singh KK, Tripathi VK, Sarkar PK. Experimental study of CFRP patches bonded on a cracked aluminum alloy panel. Composite Interfaces. 2015; 22(4):233-48.
[25] Grave JH, Echtermeyer AT. Strain fields in adhesively bonded patch repairs of damaged metallic beams. Polymer Testing. 2015; 48:50-8.
[26] Benyahia F, Aminallah L, Albedah A, Bouiadjra BB, Achour T. Experimental and numerical analysis of bonded composite patch repair in aluminum alloy 7075 T6. Materials & Design. 2015; 73:67-73.
[27] Beloufa HI, Ouinas D, Tarfaoui M, Benderdouche N. Effect of stacking sequence of the bonded composite patch on repair performance. Structural Engineering and Mechanics. 2016; 57(2):295-313.
[28] Reburn A. Analysis of manufacturing parameters on the shear strength of aluminium/GFRP co-cured and adhesively bonded single-lap joints. The Plymouth Student Scientist. 2016; 9(2):195-230.
[29] Ribeiro TE, Campilho RD, Da SLF, Goglio L. Damage analysis of composite–aluminium adhesively-bonded single-lap joints. Composite Structures. 2016; 136:25-33.
[30] Vishnuvardhan NL, Pathak H, Singh A. Composite patch repair modelling by FEM. In proceedings of first structural integrity conference and exhibition 2016 (pp. 4-6).
[31] Ungureanu D, Taranu N, Lupasteanu V, Rosu AR, Mihai P. The adhesion theories applied to adhesively bonded joints of fiber reinforced polymer composite elements. The Bulletin of the Polytechnic Institute of Lasi, Department of Construction, Architecture. 2016; 62(2):37.
[32] Turan K, Örçen G. Failure analysis of adhesive-patch-repaired edge-notched composite plates. The Journal of Adhesion. 2017; 93(4):328-41.
[33] Ramakrishna C, Balu JK, Rajashekar S, Sivateja N. Finite element analysis of the composite patch repairs of the plates. International Journal of Engineering Research and Application. 2017; 7(2):10-8.
[34] Shinde PS, Kumar P, Singh KK, Tripathi VK, Aradhi S, Sarkar PK. The role of yield stress on cracked thin panels of aluminum alloys repaired with a FRP patch. The Journal of Adhesion. 2017; 93(5):412-29.
[35] Budhe S, Banea MD, De BS, Da SLF. An updated review of adhesively bonded joints in composite materials. International Journal of Adhesion and Adhesives. 2017; 72:30-42.
[36] Echer L, Marczak RJ, De SCE. Studies on repair patch shapes optimization for damaged composites. Proceedings of the XXXVIII Iberian Latin-American congress on computational methods in engineering 2017.
[37] Aityala A, Demouche N, Beddek S, Hamid K. Full analysis of all composite patch repairing design parameters. Iranian Journal of Materials Science & Engineering. 2018; 15(4).
[38] Özer H. Introductory chapter: structural adhesive bonded joints. Applied Adhesive Bonding in Science and Technology. 2018.
[39] Fernandes RL, Campilho RD. Accuracy of cohesive laws with different shape for the shear behaviour prediction of bonded joints. The Journal of Adhesion. 2019; 95(4):325-47.
[40] Aabid AB, Hrairi M, Ali JS, Abuzaid A. Effect of bonded composite patch on the stress intensity factors for a center-cracked plate. IIUM Engineering Journal. 2019; 20(2):211-21.
[41] Li C, Zhao Q, Yuan J, Hou Y, Tie Y. Simulation and experiment on the effect of patch shape on adhesive repair of composite structures. Journal of Composite Materials. 2019; 53(28-30):4125-35.
[42] El-sagheer I, Taimour M, Mobtasem M, Abd-elhady A, Sallam HE. Finite element analysis of the behavior of bonded composite patches repair in aircraft structures. Fracture and Structural Integrity. 2020; 14(54):128-38.
[43] Garg N, Prusty BG, Ooi ET, Song C, Pearce G, Phillips AW. Application of scaled boundary finite element method for delamination analysis of composite laminates using cohesive zone modelling. Composite Structures. 2020; 253:112773.
[44] Garg N, Chakladar ND, Prusty BG, Song C, Phillips AW. Modelling of laminated composite plates with weakly bonded interfaces using scaled boundary finite element method. International Journal of Mechanical Sciences. 2020; 170:105349.
[45] Yousefi A, Mosavi MM, Safarabadi M. Numerical analysis of cracked aluminum plate repaired with multi-scale reinforcement composite patches. Journal of Composite Materials. 2020; 54(28):4341-57.
[46] De OLA, Donadon MV. Delamination analysis using cohesive zone model: a discussion on traction-separation law and mixed-mode criteria. Engineering Fracture Mechanics. 2020; 228:106922.
[47] Wciślik W, Pała T. Selected aspects of cohesive zone modeling in fracture mechanics. Metals. 2021; 11(2):1-15.
[48] Echer L, Souza CE, Marczak RJ. A study on the best conventional shapes for composite repair patches. Materials Research. 2021; 24(Suppl 2):e20210304.
[49] Amari K, Berrahou M. Experimental and numerical study of the effect of patch shape for notched cracked composite structure repaired by composite patching.

Journal of Failure Analysis and Prevention. 2022; 22(3):1040-9.
[50] Benkheira A, Belhouari M, Madani K, Gong XL. Experimental and numerical study of the effect of debonding defect in composite patch repairs on composite plate. Journal of Failure Analysis and Prevention. 2022; 22(4):1669-92.
[51] Berrahou M, Amari K. Numerical analysis of the repair performance of notched cracked composite structure repaired by composite patch. Journal of Materials and Engineering Structures. 2022; 9(3):317-26.
[52] Tamboli S, Pandey A, Patil MV. Investigation and optimisation of cracked aluminium alloy plate restored for fatigue loading application. International Journal of Computer Aided Engineering and Technology. 2022; 16(2):153-69.
[53] Aabid A, Ibrahim YE, Hrairi M, Ali JS. Optimization of structural damage repair with single and double-sided composite patches through the finite element analysis and Taguchi method. Materials. 2023; 16(4):1-14.
[54] Shinde H, Kumar P, Karnik M, Sonawane N. Numerical simulation of pre-cracked thin aluminum alloy skin repaired with a FRP patch: pre-crack length studies. Materials Today: Proceedings. 2023; 72:1774-9.
[55] Khode AP, Nimje SV. Numerical simulation for stress analysis of functionally graded adhesively bonded composite patch repair system. Discover Mechanical Engineering. 2023; 2(1):15.
[56] Abdelfattah I, Ferreira F, Nasr SM, Reis PN, Teixeira DFS. Flexural performance of squared one-sided CFRP patches: modelling and experimental study. The Journal of Adhesion. 2023; 99(3):473-91.
[57] Luo GM, Liang CH. Strength verification of a carbon-fibre-reinforced plastic patch used to repair a cracked aluminium alloy plate. Applied Composite Materials. 2024; 31(1):265-89.
[58] Rasane AR, Kumar P, Khond MP. Optimizing the size of a CFRP patch to repair a crack in a thin sheet. The Journal of Adhesion. 2017; 93(13):1064-80.
[59] Rasane AR. Repair of a thin structural sheet using polymer composite patches. Ph.D. Thesis, Savitribai Phule University, Pune. 2019.
[60] Rasane A, Kumar P, Khond M. Analysis of the failure of bonded interface between aluminium skin and FRP patch using cohesive zone model. Journal of The Institution of Engineers (India): Series C. 2019; 100:869-78.

Amol Rasane was born in Nashik, Maharashtra, India, in 1980. He received his Bachelor's and Master's degrees in Mechanical Engineering from the University of Pune, India, in 2001 and 2011, respectively. He earned a Ph.D. in Mechanical Engineering from the University of Pune in 2019. He is currently working as an Assistant Professor of Mechanical Engineering at PVG's College of Engineering & S.S. Dhamankar Institute of Management, Nashik, India. He has obtained Level-1 certification in TRIZ, and his research areas include computer-aided design and manufacturing. Dr. Rasane is a life member of the Indian Society for Technical Education, a life member of the Indian Society for Manufacturing Engineers, and an Associate of the Institution of Engineers (India).
Email: ramolr2003@yahoo.co.in

Prashant Kumar received B.Tech degree in Mechanical Engineering from Indian Institute of Technology, Kanpur (India). He obtained M. Tech degree in Design from University of California (USA) and Ph.D. in Mechanics of Solids from Brown University (USA). He was associated with Indian Institute of Technology, Kanpur as a teaching faculty. He has over three decades of teaching and research experience. He has published a number of papers in national/ international journals and magazines. He has worked on sponsored projects on fracture aspects of polymer composites. He has been a consultant to many industries around Kanpur and national organizations like HAL Korwa, ADE Bangalore and ADA Bangalore.
Email: prkumar@iitk.ac.in

Mohan Khond was born in Yavatmal district, Maharashtra, India. He received his Bachelor's degree in Mechanical Engineering from Amravati University in 1989, his Master's degree in Mechanical Engineering from Devi Ahilya Vishwavidyalaya in 1994, and his Ph.D. in Mechanical Engineering from Amravati University in 2008. He has been working as an Associate Professor of Mechanical Engineering at COEP Technological University since 2003. He is currently serving as the Dean of Student Development at COEP Technological University.
Email: mpk.mech@coep.ac.in

Appendix I

S. No.	Abbreviation	Description
1	CFRP	Carbon Fiber Reinforced Polymer
2	CZM	Cohesive Zone Material
3	FEM	Finite Element Method
4	G_I	Energy Release Rate in mode-I
5	G_{II}	Energy Release Rate in Mode-II
6	G_{Ic}	Critical Energy Release Rate in Mode-I
7	GFRP	Glass-Fiber-Reinforced-Polymer
8	G_{IIc}	Critical Energy Release Rate in Mode-II
9	LE, G	Leading Edge of Glass Fiber Layer
10	LE, C	Leading Edge of Carbon Fiber Layer
11	MMC	Mixed-Mode-Criterion
12	SIF	Stress Intensity Factor